Hybrid laser and subtractive machining of reaction bonded silicon carbide

M. Groeb[1], R. Catrin[1], J. Groeb[2]
[1]*RhySearch, Buchs, Switzerland*
[2]*Independent Researcher, Darmstadt, Germany*

Abstract

The use of high-performance materials such as technical ceramics is rapidly increasing, as these materials have many advantageous properties. The high hardness, high resistance to chemical and abrasive wear, high young's modulus and low weight are proving their use in creating complex, more precise and efficient machinery and mechanisms. The high hardness coupled with the low surface energy make mechanical finishing of these materials highly time consuming and therefore expensive. In this study, reaction bonded silicon carbide (RB-SiC) is pre-machined with an ultra-short pulse laser to create periodic fracture zones, enabling higher material removal modes. Finishing is performed in a ductile cutting regime, leading to better surface finishes, less breakouts and tighter tolerance control. For this, several experiments based on a Design of Experiments plan are undertaken, varying the pulse energy, dwell time of the laser, but also the cutting parameters of the milling tool such as median chip thickness and cutting speed. During the experiments, the specific cutting energy was monitored via a dynamometer. After the cutting trials, the surfaces were analysed via white light interferometry. A significant reduction in the specific cutting energy with laser pre-damage was achieved.

1 Introduction

The ever-increasing demands of high-technology industries such as semiconductor, chemical, aerospace but also medical and precision engineering fields have pushed traditional materials such as steels or titanium towards their theoretical limits. Novel and future applications are characterized by higher chemical and physical loads, increased demands to metrological stability, requiring higher stiffnes, hardness, chemical and temperature stability but also

lower thermal expansion coefficients [1-3]. Technical ceramics such as zirconia oxide (ZrO_2), silicon carbide (SiC), alumina oxide (Al_2O_3) but also silicon nitride (Si_3N_4) are able to fulfil these requirements. These materials are characterized by high hardness, large young's modulus, excellent temperature and chemical stability, which stems from their predominantly short sp^3-sp^3 bond length and thus their strong covalent and ionic bonds [4-7]. The manufacturing of components from these materials, especially through milling is responsible for a large part of the production cost [8-9]. The mechanical manufacturing is especially challenging, as the combination of an unfavourable young's modulus and hardness, a low ratio between tensile and shear strength but also low dislocation mobility, density and high hardness lead towards extremely brittle machining. The brittle nature in combination with the high hardness increases tool wear, allowing only for diamond machining of these substrates [10]. Laser machining inherently offers the promise of machining with no tooling cost but is characterized by low material removal rates. Moreover, the achievable surface finish with laser ablation machining can be considered low. This research focuses on a hybrid process between a femto second short pulse laser and a high precision milling machine. For this, the laser is ablating localized damages into the material, thus lowering the required cutting energy in the milling operations.

2 Materials and Methodology

In the experiments, a sintered commercial grade silicon carbide ceramic was used. The ceramic was produced by FCT Ingenieurkeramik GmbH, Germany. Table 1 shows the composition as well as material characteristics.

Table 1: Material characteristics.

Density	Grain Size	Hardness	Young's Modulus	Tensile Strength	Sinteradditive
>3.12 g/cm^3	1-10 µm	28 GPa	450 MPa	3.0 MPam$^{1/2}$	C/B_4C

To explore the idea of pre-damaging the material, but also analyse the influencing parameters, a number of experiments were carried out:

I. Scoping Laser Experiments to explore the depth and size of the laser ablation in the material
II. Milling experiments in the undamaged material to establish a baseline comparison for the specific cutting energy
III. Milling experiments in the pre-damaged material to explore the potential benefits in a hybrid process

All laser experiments were performed on a GFH (Deggendorf, Germany) laser material processing centre GL.compact II featuring an ultrashort pulse laser source (Carbide by Light Conversion) with pulse duration ranging 250 fs – 10 ps.

A wavelength of 1030 nm was used. The laser material processing centre features a five-axis simultaneous motion system, thermal control of all machine components and a state-of-the-art computer numeric control system. The laser beam was focused with a F_{theta} lens of 60 mm focal length, which produces a beam with a diameter of approximately 28 µm. The laser pulse duration was fixed to 309 femtoseconds at a repetition rate of 100 kHz. Compressed air was additionally used during the laser machining at a fixed pressure of 3 bar. In the experiments, the effect of different laser exposure times and energies were analysed. Table 2 sums up the used experimental settings for the laser machining. The depth of the laser damage was measured optically on a white light interferometer (S-Neox, Sensofar, Spain)

Table 2: Experimental settings of the laser machine.

Parameter	Level 1	Level 2	Level 3
Laser energy / µJ	50	100	170
Laser fluence / J/cm^2	8.1	16.2	27.6
Dwell Time	10	20	50

All milling experiments were undertaken on a high precision milling machine (Kern Micro HD, Kern Microtechnik GmbH, Germany). The machine is equipped with an HSK 40 high speed spindle (Fischer MFW1224, 42.000 min^{-1}, 15.6 kW), hydrostatic guideways and a central temperature control system, allowing for positional accuracies in the sub-micron range. All milling experiments were performed under flood coolant (Oelheld SintoGrind TC-X 1500). Special attention was taken to enable comparable results during the experiment series. For this, the machine was warmed up according to the manufacturers specification and the used material was prepared for the experiments by milling test structures in a ductile cutting regime.
All cutting experiments used a lasered, multi flute, poly-crystalline cutting tool manufactured by Zecha Hartmetall-Werkzeugfabrikation GmbH (Germany). The tool (see figure 1) has a diameter of 3 mm with 22 cutting edges and a corner radius of 0.03 mm.

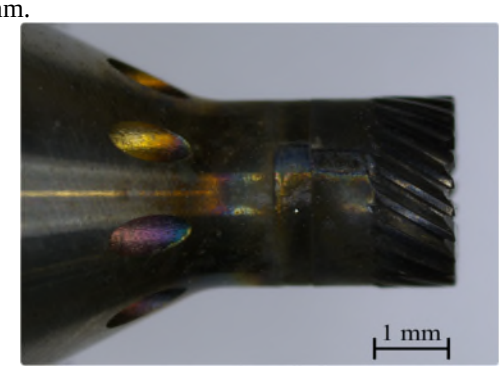

Figure 1: The used PCD Endmill, manufactured by Zecha.

During the cutting experiments, the cutting force was measured via a dynamometer plate (MiniDyn Type 9119AA2, Kistler, Switzerland), which was held in a vise. The force data was recorded with a high resolution charge amplificator (LV Type 5080A) connected to a digital analogue converter (DAQ Type 5697A). Figure shows the experimental setup on the milling machine.

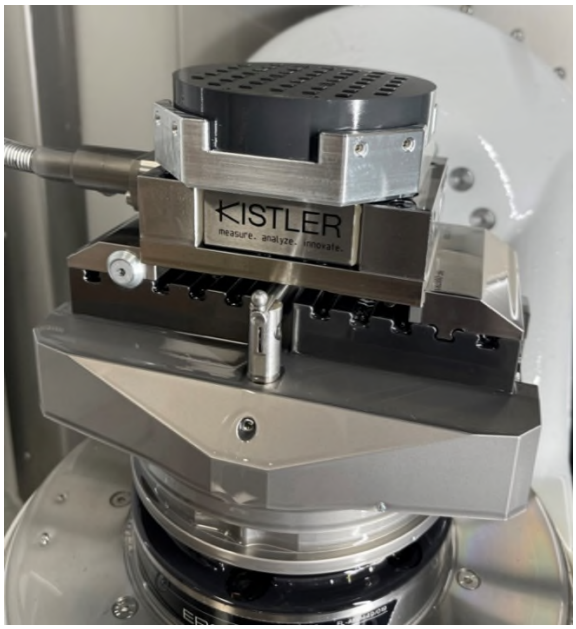

Figure 2: The experimental setup on the milling machine.

Afterwards, the cutting torque and specific cutting energy were calculated from the force data, geometric data and spindle rotational speed. The calculation and evaluation was performed with Python 3.9.

In order to reduce extraneous influences and generate the maximum information output from the experiment series, the cutting and laser trials were conducted with a Design of Experiments approach, utilising Taguchi based orthogonal experiment matrixes.

3 Experimental Study

The first experiment series explored the interaction depth and diameter of the laser beam with the material. For this, the experimental parameters (compare table 3) were varied to create 9 different laser settings. Table 4 shows the experimental combinations. By using different dwell times and laser power settings, the depth of the created holes can be adjusted. The holes were evenly spaced along the pre-milled structures. After the experiments, a row of holes was partially milled open by side milling on the high-precision milling machine. By using a zero-point

clamping system, the sample specimen could be switched between the two machines without loss of reference. By partially opening the holes, an accurate measurement of the hole depth and diameter on the white light interferometer is enabled.

Table 3: Experimental settings of the first experiment series.

Run #	**Dwell time / ms**	**Laserpower / µJ**
LD_1	10	50
LD_2	10	100
LD_3	10	170
LD_4	20	50
LD_5	20	100
LD_6	20	170
LD_7	50	50
LD_8	50	100
LD_9	50	170

The second experiment series established a base line for the milling experiments in the undamaged stock material. For this, a number of experimental settings (see table 4) were analysed via force measurements on the high-precision milling machine. During the cutting trials, the median chip thickness (Hm) and the cutting depth was varied. The parameters of the cutting depth are matched with the average hole depth in the different laser parameter trials. The recorded cutting force data is used to calculate via the torque and rotational spindle speed the specific cutting power.

Table 4: Experimental settings of the second experiment series.

Experiment Number	1	2	3	4	5	6	7	8	9
Milling Depth / µm	80	100	150	200	300	400	80	100	150
Hm / nm	50	50	50	50	50	50	100	100	100
Experiment Number	10	11	12	13	14	15	16	17	18
Milling Depth / µm	200	300	400	80	100	150	200	300	400
Hm / nm	100	100	100	150	150	150	150	150	150

In the third experiment series, the material was pre-damaged with the short-pulse laser and then side-milled. Table 6 shows the experimental settings of both the milling machine and the laser centre.

4 Results and Analysis

The first experiment series explored the interaction of the laser with the material. By dwelling the laser for a certain time over the material, cylindrical holes are formed. Interferometric measurements have shown that the hole diameter is 29 µm, which is approximately equal to the laser spot size, with negligible deviation from a cylindrical from. Figure 3 shows a close up of the lasered holes.

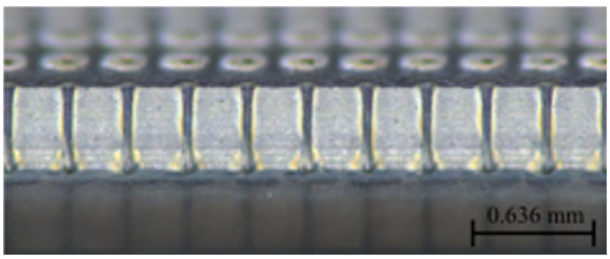

Figure 3: An optical micrograph of the lasered and through side milling opened holes.

By evaluating the lasered structures after side milling the holes have open, the depth of each individual laser setting could be measured. For this, 8 damage zones were measured under the white light interferometer. Table 5 lists the achieved depth. Remarkably, the achieved depth shows only a small amount of variation.

Table 5: Experimental settings of the laser machine.

Trial Number	1	2	3	4	5	6	7	8	9
Achieved Depth / µm	80	95	140	100	150	200	200	300	400
Std. Deviation / µm	10	8	11	7	9	11	8	10	11

The evaluated depths were later used to set the milling depth in the third experiment series.

The second experiment series established a baseline for the specific cutting energy. For this, several fields at different depths and median chip thickness settings were milled. The third experiment series milled with identical cutting parameters in the pre-damaged material. Table 6 shows the experimental settings and resulting specific cutting energies. For better comparability, both experiment series are evaluated in the following together.

Table 6: Experimental parameters for the pre-damaged trials. W_s is the spacing between the laser damages, T_d the dwell time, P_L the laser power, DOC the depth of cut, Hm the median chip thickness, U_{s_nld} the specific cutting energy for the non-laser damaged and U_{s_ld} for the laser damaged regions.

Run N	W_s / mm	T_d / ms	P_L / µJ	DOC / µm	Hm / nm	U_{s_nld} / µJ/mm^3	U_{s_ld} / µJ/mm^3
1	0.1	10	50	80	50	161.5	93.1
2	0.1	20	100	150	100	112.6	35.1
3	0.1	50	170	400	150	60.0	32.1
4	0.2	10	50	80	100	190.3	44.1
5	0.2	20	100	150	150	87.7	29.9
6	0.2	50	170	400	50	90.0	39.8
7	0.3	10	100	100	150	113.4	48.3
8	0.3	20	170	200	50	124.5	59.7
9	0.3	50	50	200	100	97.7	52.9
10	0.1	10	170	150	100	112.6	25.4
11	0.1	20	50	100	150	113.4	28.5
12	0.1	50	100	300	50	101.1	29.5
13	0.2	10	100	100	50	169.2	64.9
14	0.2	20	170	200	100	97.7	43.0
15	0.2	50	50	200	150	78.1	34.3
16	0.3	10	170	150	150	87.7	28.8
17	0.3	20	50	100	50	169.2	6.8
18	0.3	50	100	300	100	82.1	36.9

Figure 4 shows the specific cutting energy U_s at different median chip thicknesses (Hm). It can be seen that there is a significant difference between the laser damaged (LD) and undamaged (NLD) cutting energies. There is no discernible influence of the laser power onto the cutting energy. At lower cutting depths (80-100 µm), the difference between individual parameter sets varies more than at higher cutting depths. This is likely because of the change in cutting force vectors due to the higher ratio of the corner radius of the used tool (compare fig. 1).

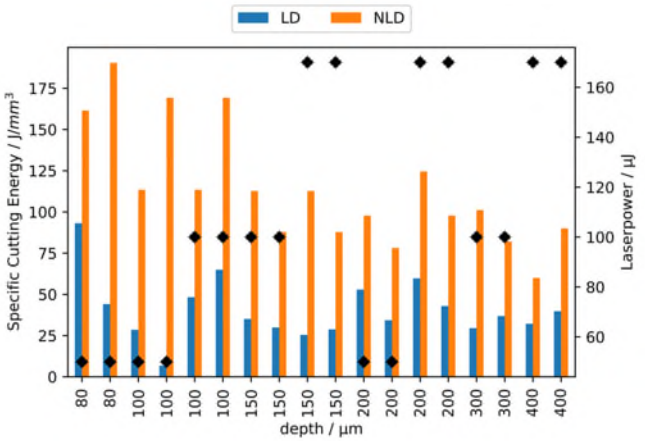

Figure 4: The specific cutting energy vs the cutting depth of the laser damaged (LD) and undamaged (NLD) cutting trials.

Comparing the specific cutting energies with the median chip thickness, it can be seen that there especially at chip thicknesses with a likely ductile cutting regime (< 100 nm), the difference in cutting energy is higher.

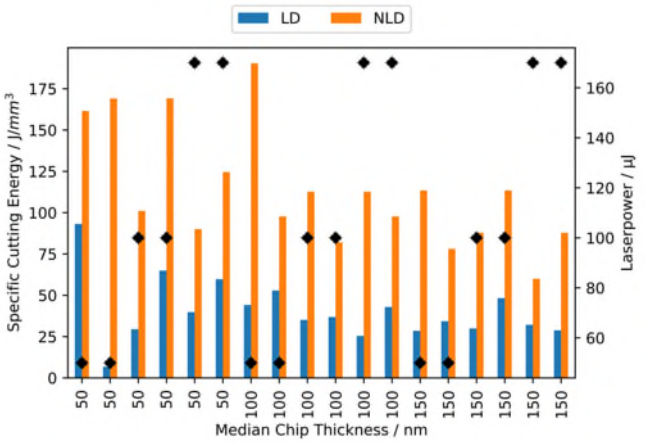

Figure 5: The specific cutting energy vs the median chip thickness of the laser damaged (LD) and undamaged (NLD) cutting trials.

This likely stems from the fact that during a ductile cutting regime, additional energy is needed for the high-pressure phase transformation, whereas in the pre-damaged material, no ductile regime can be reached before the material removal sets in. No significant influence of the point spacing on the cutting reduction could be detected. This implies that an even wider spacing could be possible, which would increase productivity of the laser operation. In general, an areal laser damaging speed of 0.5 mm2/s can be achieved.

Figure 6 shows an overview over the experiment series. It can be seen that a clear reduction of the specific cutting energy was achieved in all experiments, with an average reduction of 63%. Experiment number 17 shows a remarkable difference in the cutting energy, and should be discarded as a faulty measurement without weakening the overall experimental design.

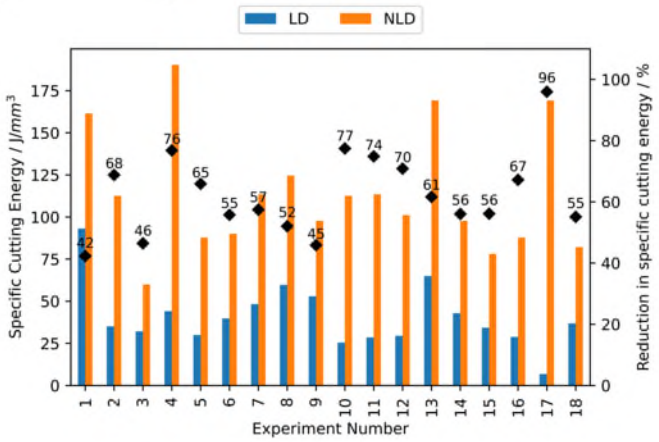

Figure 6: Overview of the experiment series with the difference in specific cutting energy between laser damaged (LD) and undamaged (NLD) cutting trials.

The significant reduction in cutting energy, independent of the damage zone spacing, especially considering that the calculated destroyed volume at 0.3 mm spacing is far below 1%, raises the question of the damaging mechanism of the laser. To explore this, SEM micrographs of the damaged zones were taken. Figure 7 shows an exemplary sample region.

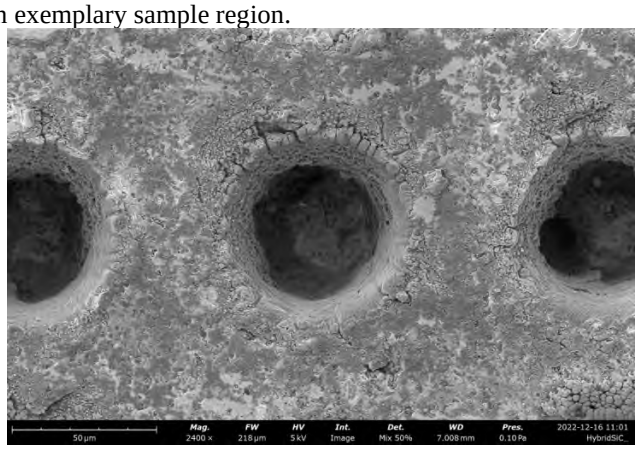

Figure 7: SEM Micrograph of the laser damaged zone. Clear melting zones, cracking and material damage is visible.

The material exhibits melting, cracking and general weakening through the laser operation. EDS analysis has shown that the melted regions are composed of SiO_2. As the material is not only damaged inside the ablated holes, but also

with a far larger reach around the damage zones, the significant reduction in cutting energy is plausible.

5 Conclusion

The trials have shown that a fast laser pre-damaging of the material is able to achieve a significant reduction of the specific cutting forces. The average reduction is 62.59%, with a standard deviation of 13.51%. SEM analysis of the surfaces have shown that no cold ablation was reached, but significant melting, cracking and weakening of the material occurred. While this usually would be inadvertent for ceramics parts, there is a large potential here for removing the inevitable additional stock on sintered parts before finishing them to high tolerances. As the depth can be relatively finely tuned through dwell time and laser power, a controlled damage of to-be-removed material can be achieved. Future research should focus on the influence of the cutting force reduction on tool life and increasing productivity, but also the exact material removal mechanism.

References

[1] Mark J. Davis und Edgar D. Zanotto. „Glass-ceramics and realization of the unobtainable: Property combinations that push the envelope“. In: *MRS Bulletin* 42.03 (2017), S. 195–199.

[2] Te Su Kwak. „A Study of Ceramic Injection Molding of Watch Case Composed of ZrO2 Powder“. In: *Materials Science Forum* 534-536 (2007), S. 337–340.

[3] Martin Schwentenwein, Peter Schneider und Johannes Homa. „Lithography-Based Cera- mic Manufacturing: A Novel Technique for Additive Manufacturing of High-Performance Ceramics“. In: *Advances in Science and Technology*. Trans Tech Publications Ltd, 2014.

[4] P. Mélinon u. a. „Playing with carbon and silicon at the nanoscale“. In: *Nature Materials* 6.7 (2007), S. 479–490.

[5] Fabrice Amy. „Atomic scale study of the chemistry of oxygen, hydrogen and water at SiC surfaces“. In: *Journal of Physics D: Applied Physics* 40.20 (2007), S. 6201–6214.

[6] *Zukunftpotenziale von Hochleistungskeramiken*. Techn. Ber. Köln: Deutsche Keramike Ge- sellschaft, 2014.

[7] Andrew John Ruys. *Alumina Ceramics: Biomedical and Clinical Applications*. Woodhead Publishing, 2018.

[8] „Ceramics Science and Technology: Volume 3: Synthesis and Processing“. In: *Ceramics Science and Technology*. Hrsg. von I-Wei Chen Ralf Riedel. Volume 3: Synthesis and Proces- sing. John Wiley und Sons, Ltd, 2011. eprint: https://onlinelibrary.wiley.com/ doi/pdf/10.1002/9783527631957.fmatter.

[9] Jürgen Rödel u. a. „Development of a roadmap for advanced ceramics: 2010–2025“. In: *Journal of the European Ceramic Society* 29.9 (2009), S. 1549–1560.

[10] John Patten, Harish Cherukuri und Jiwang Yan. „Ductile-regime machining of semiconduc- tors and ceramics“. In: *High pressure Surface Science and Engineering* (2003), S. 639.